frontiers | Frontiers in Materials

TYPE Original Research
PUBLISHED 13 November 2024
DOI 10.3389/fmats.2024.1509077



OPEN ACCESS

EDITED BY
Biao Hu,
Shenzhen University, China

REVIEWED BY
Cong Lu,
Southeast University, China
Yanshuai Wang,
Shenzhen University, China

*CORRESPONDENCE
Qingxin Zhao,
l1220805317@qq.com

RECEIVED 10 October 2024
ACCEPTED 28 October 2024
PUBLISHED 13 November 2024

CITATION
Wang H, Li C, Gao H, Zhao Y, Xia H, Zhou C, Zhong S and Zhao Q (2024) Improvement of dispersants on nano carbon black-modified cement paste: performance, microstructure and carbon footprint.
*Front. Mater.* 11:1509077.
doi: 10.3389/fmats.2024.1509077



# Improvement of dispersants on nano carbon black-modified cement paste: performance, microstructure and carbon footprint

Hui Wang[1], Chenjiang Li[2], Haixiang Gao[1], Yan Zhao[3], Handuo Xia[3], Cong Zhou[1], Shunjie Zhong[4] and Qingxin Zhao[5]*

[1]Cangzhou Qugang Expressway Construction Co., Ltd., Cangzhou, China, [2]State Key Laboratory of Hydraulic Engineering Intelligent Construction and Operation, Tianjin University, Tianjin, China, [3]China Mcc22 Group Corporation Ltd., Tangshan, China, [4]Fujian Zhanglong Construction Investment Group Co., Ltd., Zhangzhou, China, [5]State Key Laboratory of Metastable Materials Science and Technology, Yanshan University, Qinhuangdao, China

The agglomeration of nano carbon black (NCB), driven by its high specific surface energy, limits the fundamental performance of cementitious materials and hinders the broader application of functional cementitious materials in engineering domains. NCB-modified cement (NC) has a low snow-melting efficiency, resulting in high energy consumption and excessive $CO_2$ emissions. Herein, this study innovatively proposed a method of using dispersants to overcome the above issue and systematically introduced the effects of three dispersants, polycarboxylic acid superplasticizer (PCE), tannic acid (TA), and sodium dodecyl sulfate (SDS), on NC. The dispersity of dispersant-NCB suspension was analyzed firstly, and then the performance of fresh paste, mechanical properties, resistivity, snow-melting speed and LCA of NC were explored. Experimental results indicated that, in terms of suspension stability, SDS was the most effective, followed by TA, while PCE exhibited the least efficacy. Furthermore, all three dispersants improved the fluidity of NC to varying degrees. However, PCE and TA demonstrated a retardation effect on the setting time, whereas SDS facilitated a reduction in the setting time of NC. From the point of view of mechanical properties, the use of these dispersants not only augmented the mechanical strength of the NC but also decreased its electrical resistivity. The uniform dispersion of SDS at the microstructural level of NCB had also been found. When the PCE content is 0.2%, TA content is 0.4%, and SDS content is 0.4%, the mechanical strength and resistivity of NC were the best. NC with dispersant TA melted snow three times faster than the control group, reducing snow-melting energy consumption. Moreover, LCA analysis showed that the addition of dispersants also reduced carbon emissions.

KEYWORDS

**nano carbon black, cement paste, dispersant, electrical properties, $CO_2$ emissions**

# 1 Introduction

In winter, high altitude areas of north and west China face significant challenges due to seasonal temperature changes and heavy snowfall, which increase snow thickness and lead to frequent icing on roads, bridges, and airports (Li et al., 2022; Julitta et al., 2014). Early snowfall and melting can create thin layers of frozen ice on highways and runways, reducing friction and posing safety risks as these surfaces can appear similar to wet roads (Wang et al., 2022). If not addressed promptly, this ice can severely impede vehicle movement, causing traffic paralysis and complicating infrastructure maintenance, accompanied by high costs (Pytka, 2010). To tackle these issues, various deicing and snow melting technologies have been employed (Zhao et al., 2024; Xu et al., 2021; Ma et al., 2016; Huang et al., 2021; Pei et al., 2021). Mechanical deicing and snow removal methods are effective but resource-intensive, while traditional salt-sprinkling methods can lead to environmental pollution and damage to concrete surfaces, including corrosion of steel in bridges. Therefore, there is an urgent need for efficient and environmentally friendly deicing solutions that can reduce reliance on human resources and minimize the negative impact on the durability of road structures and bridges.

In recent years, the emergence of multi-functional cement-based materials has also provided new ideas for solving road engineering problems (Zhai et al., 2023; Zhan et al., 2020; Han et al., 2015). As a multi-functional cement-based material, electro-thermal concrete has been used in the field of deicing and snow-melting of pavement due to its good mechanical properties and excellent electric heating ability. The excellent electrothermal property of electro-thermal concrete is reflected in the fact that it can heat up buildings or concrete pavement by external power supply voltage in winter snow and ice weather, so that the temperature rises and maintains a relatively stable value, so that the buildings or pavement can be kept in a state without snow and ice in a long period of cooling and snowfall weather, which can effectively prevent adverse situations (Li et al., 2013). Over the past decade or so, carbon materials have attracted much attention due to their high specific surface area and high strength. A large number of studies have shown that the addition of carbon materials to cement-based materials can greatly improve their mechanical and electrical properties, such as carbon nanotubes (Pan et al., 2020; Yıldırım et al., 2018), graphene (Bai et al., 2018; Yoo et al., 2017; liu et al., 2019) and nano carbon black (NCB) (Gong et al., 2009; Hong et al., 2018; Keal et al., 2024), etc., which are often used as fillers for conductive concrete. In contrast, NCB is a more cost-effective option and has a very broad practical application prospect. In addition, studies have shown that NCB can not only effectively repair micro-cracks in cement, but also accelerate the hydration degree of cement, thereby improving the mechanical properties of cement.

However, due to the high specific surface energy of NCB, it is easy to aggregate under the action of van der Waals force (Geim and Novoselov, 2007; Zhu et al., 2010; Chuah et al., 2018), and the direct addition of NCB often leads to poor fluidity and low mechanical strength of cement-based materials (Sobolkina et al., 2012; Xu et al., 2018). The low snow-melting efficiency of NC has led to increased electricity consumption, resulting in a significant amount of $CO_2$ emissions. In order to avoid the restriction of caking when NCB is applied in cement, a uniform and stable dispersion is required. Many researchers have conducted a lot of research, and currently there are two main dispersion treatment methods: physical dispersion (Nan et al., 2023) and chemical treatment (Kishore et al., 2023). Physical dispersion technology usually uses grinding, ball milling, ultrasonic and microwave radiation methods to achieve uniform suspension of particles. Although the physical technology is simple and fast, it also has a big disadvantage: it is not enough to achieve long-term stable dispersion. The chemical treatment technology is mainly to modify the particles by surfactants and realize non-covalent functionalization to improve their hydrophilicity, so that the particles can be stably dispersed into the solvent. In summary, how to improve the dispersion stability of NCB in cement hydration environment and reduce the $CO_2$ emissions from NC snow-melting have become key problems. Therefore, it is particularly important to disperse NCB better, improve its application effect in cement-based materials and reduce the $CO_2$ emissions from NC snow-melting.

Based on the existing problems, and in order to better play the application of NCB in cement-based materials, three different surfactants, sodium dodecyl sulfate (SDS), polycarboxylic acid superplasticizer (PCE) and tannic acid (TA), were selected as dispersants to disperse NCB. Starting with NCB suspension, the effects of three dispersants on the dispersion stability of NCB in aqueous solution were investigated by ultraviolet spectrophotometry. Subsequently, the performance of NC was investigated, and the influence of three dispersants on the new mixing performance of NC was demonstrated according to the test of fluidity and setting time. Then, on the surface of NC, the effects of three dispersants on the physical and electrical properties of NC were analyzed by compressive and flexural strength and resistivity tests. The effect of SDS on the microstructure of NC-paste also been studied. Finally, the snow-melting speed of NC with different dispersants was studied through the test of snow-melting. Meanwhile the life cycle assessment of each group was made to judge their $CO_2$ emissions. The reliable experimental data were obtained, which laid a foundation for practical engineering application.

# 2 Material and methods

## 2.1 Raw materials

The cement was P.O 42.5 ordinary Portland cement produced by Tianjin Jinyu Zhenxing Cement Factory, and its chemical composition is shown in Table 1. Carbon black was NCB with high specific surface area and low resistivity provided by Tianjin Huaran Chemical Co., LTD. NCB was prepared by gas phase method, and its related performance parameters are shown in Table 2. The dispersant SDS was from Shanghai Sigma Aldrich Trading Co., LTD. The water reducing agent was the third generation PCE with water reduction rate ≥25%. The purity of TA used was AR grade, provided by Hunan Beekman Biotechnology Co., LTD. For the convenience of reading, the abbreviations in this article are summarized in Table 3.

## 2.2 Sample preparation

In order to better study the modification effect of various dispersants on NCB cement-based composites, cement paste

TABLE 1 Chemical composition of cement (%).

| CaO | $SiO_2$ | $Al_2O_3$ | $Fe_2O_3$ | MgO | $SO_3$ | $K_2O$ | Loi |
|---|---|---|---|---|---|---|---|
| 62.8 | 21.56 | 4.67 | 3.31 | 2.38 | 3.25 | 1.25 | 0.78 |

without coarse or fine aggregate was used in this study. The water-cement ratio of the cement-based composite prepared by the test is fixed at 0.45. The specific ratio is shown in Table 4. Firstly, a suspension of dispersant mixed with NCB was prepared, and then the NCB suspension was prepared for the preparation of cement paste.

(1) Preparation of dispersant-NCB suspension: Take the preparation standard of NCB/SDS solution as an example to illustrate (PCE and TA preparation methods were consistent with SDS). Firstly, 0.1 g NCB and 50 mL SDS solution with different mass fractions (0%, 0.2%, 0.4%, 0.6%) were added into 100 mL beaker, mechanically stirred for 5 min and ultrasonic dispersion for 15 min to obtain NCB/SDS suspension.
(2) Preparation of cement paste sample: A total of 300 mL of PCE/TA/SDS and NCB suspensions were prepared, mechanically stirred for 5 min, and ultrasonically dispersed for 15 min. Weighed cement was added to the mixer, followed by the 300 mL NCB suspension, and mixed for 1.5 min. After a 30-second pause, 264 g of water was gradually added while stirring, and mixing continued for another 1.5 min. The paste was then poured into a lubricated steel mold (40 × 40 × 160 mm). After shaking for 30 s, the surface was covered with polyethylene film to prevent water loss. The mold was removed after 24 h and placed in a standard curing room for further testing.

The preparation method of the specimen for the electrical conductivity test was roughly the same as that for the mechanical properties of the specimen, the only difference was that the electrical conductivity test uses the four-electrode method to determine the resistivity, so it was necessary to prepare 40 × 50 mm copper mesh as the measuring electrode.

## 2.3 Test methods

### 2.3.1 Absorbance test

The dispersion of dispersant NCB suspension was evaluated by ultraviolet spectrophotometry. The PE Lambda 750 s spectrophotometer was selected to measure the absorbance (ABS) within 24 h at 270 nm wavelength (Lavagna et al., 2021). The test mix ratio was consistent with that described in Section 1.3. The strength of absorbance can be expressed by the following Formula 1:

$$A = Kbc \tag{1}$$

where: A is absorbance; K is the molar absorption coefficient, which is related to the properties of the absorbing material and the wavelength λ of the incident light. b is the thickness of the absorption layer; c is the concentration of the light-absorbing substance in mol/L. In this test, the molar absorption coefficient K and the thickness of the absorption layer b are fixed. At this time, the absorbance A of the solution is positively correlated with the concentration c of the dispersant in the suspension, which can be used to quantitatively describe the dispersion effect of NCB in the solution.

### 2.3.2 Fresh cement paste performance test

In order to determine the effect of dispersant on the new mixing performance of NC, the fluidity and initial and final setting time of paste at room temperature (20°C ± 2°C) were measured by NLD 3 electric cement paste fluidity tester and Vicar meter. For specific test steps, refer to GB/T 1346–2011 "Test Method for Water Consumption, Setting Time and Stability of Cement Standard Consistency", the test was carried out three times, and the average value was taken as the test result.

### 2.3.3 Mechanical properties test

YAW-300C automatic bending testing machine was used to measure the compressive strength and flexural strength of the specimens, and the test method in GB/T17671-1999 "Cement mortar Strength Inspection Method (ISO method)" was used as the standard.

### 2.3.4 Electrical performance test

The main function of conductive phase filler NCB was to significantly improve the electrical conductivity of cement-based materials, and the direct measurement of sample resistance by instrument and electric meter was easy to produce a large error. Therefore, the four-electrode method was selected to measure the resistivity of the sample in this experiment. The current and voltage were measured by the multifunctional electric meter produced by Tianlilong Technology Co., LTD. The DC regulated power supply provided by Youlide was used as the voltage input terminal. The copper mesh was provided by Hebei Hengshui Furun Filter Co., LTD., with a diameter of 0.7 mm and low error and resistivity. The four-electrode measurement method is shown in Figure 1. The test piece was subjected to direct current of 0 ~ 30 V to measure its voltage and current, and the resistivity of early and late hydration was calculated by Formula 2, 3.

The calculation formula is as follows:

$$R = \frac{U}{I} \tag{2}$$

$$\rho = \frac{RS}{L} \tag{3}$$

Where: U represents the actual measured voltage, V; I represents the actual measured current, mA; R represents the calculated resistance between the middle two electrodes, Ω; rrepresents the resistivity of the sample, Ω·cm; L represents the distance between the middle two electrodes, mm; S represents the cross-sectional area of the sample, $mm^2$.

### 2.3.5 Snow-melting test

Snow-melting test was to observe the change of ice mass with time under certain temperature conditions. First, add 100 g of water into the beaker and freeze it in the refrigerator at −18°C for more than 12 h until the water was completely frozen. The ice cube was a cylinder with a diameter of 30 mm on the bottom side. The ice

TABLE 2 NCB performance index.

| Particle size (nm) | Iodine absorption value (g/kg) | D.B.P absorption value (ml/100 g) | Electrical resistivity (Ω•m) | pH | Heating decrement (%) | Ash content (%) | Ctab surface area (m2/g) | Impurity |
|---|---|---|---|---|---|---|---|---|
| 30 | 820 | 380 | 0.9 | 7.2 | 0.2 | 0.1 | 150 | no |

TABLE 3 Description of abbreviations used.

| Abbreviation | Description |
|---|---|
| NCB | Nano carbon black |
| NC | NCB-modified cement |
| PCE | Polycarboxylic acid superplasticizer |
| TA | Tannic acid |
| SDS | Sodium dodecyl sulfate |
| SEM | Scanning electron microscopy |
| XRD | X-ray diffraction |
| AFt | Ettringite |
| C-S-H | Calcium Silicate Hydrate |

cube was placed in the middle of the specimen, and the voltage was connected to each group of NC in the same way as the electrical performance test. Quickly measure the mass of the ice every 5 min. High snow-melting efficiency led to lower electricity consumption and reduced $CO_2$ emissions.

### 2.3.6 Microscopic characterization tests

Scanning electron microscopy (SEM) was employed to analyze the microscopic distribution of NCB. Specimens measuring 10 mm × 10 mm × 10 mm were cut from the cement paste and vacuum-dried to avoid carbonation from $CO_2$ exposure. The dried samples were then subjected to SEM testing after being coated with gold. The Czech TESCAN MIRA LMS was utilized for the SEM analysis and energy spectrum testing. X-ray diffraction (XRD) was used to determine the crystalline structure of materials. The sample was finely powdered and placed on a sample stage, where X-rays were directed at it. As the X-rays interact with the crystal lattice, they produced a diffraction pattern that can be analyzed to reveal information about the crystallographic phases present in the materials.

### 2.3.7 Life cycle assessment analysis

The purpose of the life cycle assessment analysis was to analyze and evaluate the environmental load generated by NC with different dispersant, so as to facilitate the quantitative calculation and comparison the effect of different dispersants. In this paper, a process-based inventory analysis method was used to classify NC with different dispersant into four processes: raw material mining, mixing, transportation and snow-melting, and the $CO_2$ emissions of each process was quantified. Finally, the global warming potential (GWP) impact category was selected (Nayır et al., 2024), and the results of inventory analysis were quantitatively evaluated to determine the impact on the external environment.

## 3 Result and discussion

### 3.1 Absorbance of dispersant-NCB suspension

Figure 2 shows the change of absorbance of NCB suspension in each group with time after ultrasonic dispersion. The results of quantitative analysis showed that the absorbance of the suspension without dispersant was 1.732 at the beginning, and decreased significantly by 1.28 in the first 2 h and to 0.1 after 12 h, with a decrease of 94%, indicating that the dispersion and stability of pure NCB suspension were poor. The reason was that the interfacial effect between NCB and aqueous solution led to the increase of interfacial tension, and the force imbalance between solid and liquid forms clumps, resulting in the condensation of NCB. In addition, the non-polar characteristics of NCB surface limited its dispersion ability in water, and it was difficult for functional groups such as hydroxyl groups to form strong interactions with water, which further promoted the formation of clumps.

Figures 2A–C show the changes in UV-visible absorptance of NCB suspension at different concentrations of PCE, TA and SDS within 24 h. The overall curve showed that the addition of PCE, TA and SDS significantly affected the initial absorbance of suspension with the same NCB content. When the concentration of PCE was 0.2%, 0.4% and 0.6%, the absorbance was 1.777, 1.859 and 2.016, respectively. When the concentration of TA was 0.2%, 0.4%, 0.6%, the absorbance was 2.067, 2.359, 2.476. When SDS concentration was 0.2%, 0.4%, 0.6%, absorbance was 2.067, 2.259, 2.376. The results showed that PCE, TA and SDS can all improved the dispersion effect of NCB in water, PCE effect was the least, while TA and SDS effect were similar. With the increase of standing time, the absorbance of all groups decreased, but tended to balance after 12 h. In terms of suspension stability, SDS was the best, followed by TA, and PCE was the worst. The addition of SDS made the absorbance decrease slowly by about 0.55, indicating that the dispersion and stability of SDS to NCB was better than that of TA. In addition, the change of SDS concentration had little effect on the dispersion of NCB, possibly because 0.2% SDS concentration was enough to cover the dispersion of NCB, and further increasing the concentration would only lead to

TABLE 4 Sample ratios for test.

| Sample number | Cement(g) | NCB(g) | Water(g) | PCE/TA/SDS suspension (g/mL) | |
|---|---|---|---|---|---|
| | | | | Water(g) | PCE/TA/SDS(g) |
| 0 | 1,254 | 40 | 264 | 300 | 0 |
| PCE-0.2 | 1,254 | 39.5 | 264 | 300 | 0.4 |
| PCE-0.4 | 1,254 | 39 | 264 | 300 | 0.8 |
| PCE-0.6 | 1,254 | 38.7 | 264 | 300 | 1.1 |
| TA-0.2 | 1,254 | 39.6 | 264 | 300 | 0.6 |
| TA-0.4 | 1,254 | 39.1 | 264 | 300 | 1.1 |
| TA-0.6 | 1,254 | 38.6 | 264 | 300 | 1.7 |
| SDS-0.2 | 1,254 | 39.8 | 264 | 300 | 0.5 |
| SDS-0.4 | 1,254 | 39.2 | 264 | 300 | 1.1 |
| SDS-0.6 | 1,254 | 38.3 | 264 | 300 | 1.6 |

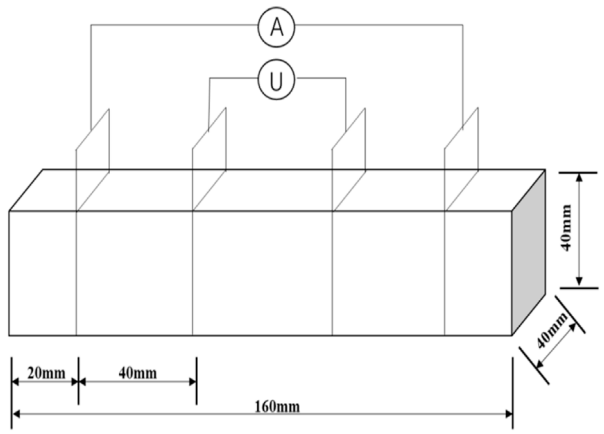


FIGURE 1
Four-electrode method.

susaturation of the solution and could not significantly improve the dispersion effect.

## 3.2 Fresh property analysis

Figures 3A–C show the flow and setting time of freshly mixed NC with different PCE, TA and SDS contents, respectively. On the whole, the three dispersants all improved the fluidity of NC to different degrees, but their performance in setting time was different.

On the whole, with the increase of dispersant content, the diffusion diameter of NC gradually increased, indicating that the addition of dispersant improved its fluidity. The diffusion diameter of the samples without dispersant was 16.8 cm, while the diffusion diameter of CPE-0.2, CPE-0.4 and CPE-0.6 increased by 20.8%, 35.1% and 59.5%, respectively. TA-0.2, TA-0.4 and TA-0.6 increased by 13.7%, 26.8% and 34.5%, respectively. SDS-0.2, SDS-0.4 and SDS-0.6 increased by 9%, 23% and 15%, respectively. It can be seen that the fluidity of PCE and TA increased with the increase of dosage, while SDS increased first and then decreased. Compared with the three dispersants, under the same dosage, PCE had the greatest improvement on fluidity, TA followed, and SDS had the least. The fluidity of PCE be due to its comb molecular structure, which formed a thicker adsorption layer, releasee free water between cement particles, and also had a certain dispersion effect on NCB. TA and SDS released encapsulated free water mainly by preventing NCB from accumulating, but TA performed slightly better in cement paste than SDS.

From the point of view of setting time, with the increase of dispersant content, the setting time of NC would be different due to the action of different dispersants. Both PCE and TA had retarding effect on NC, and TA had a more significant effect, which had also been reflected in previous Portland cement studies (Sokołowska et al., 2024). On the contrary, SDS shortened the setting time of the paste, which indicated that the action mechanism of different dispersants in NC was different. The initial and final setting times of NC without dispersant were 4.08 h and 5.33 h, respectively, while those of CPE-0.6 were 5.42 h and 6.82 h, respectively, and the time interval was slightly extended. This was because the hydroxyl, carboxyl and amino groups in PCE molecules form complexes with calcium ions in NC, which hindered the hydration process of cement. The initial and final setting times of TA-0.6 samples were 6.62 h and 8.47 h, respectively, and the time intervals were further extended, which could be explained by the theory of the formation of complexes between TA and calcium ions. In contrast, the initial and final setting time of SDS-0.6 sample were shortened to 3.65 h and 4.62 h, respectively, and the time interval was reduced, indicating that SDS

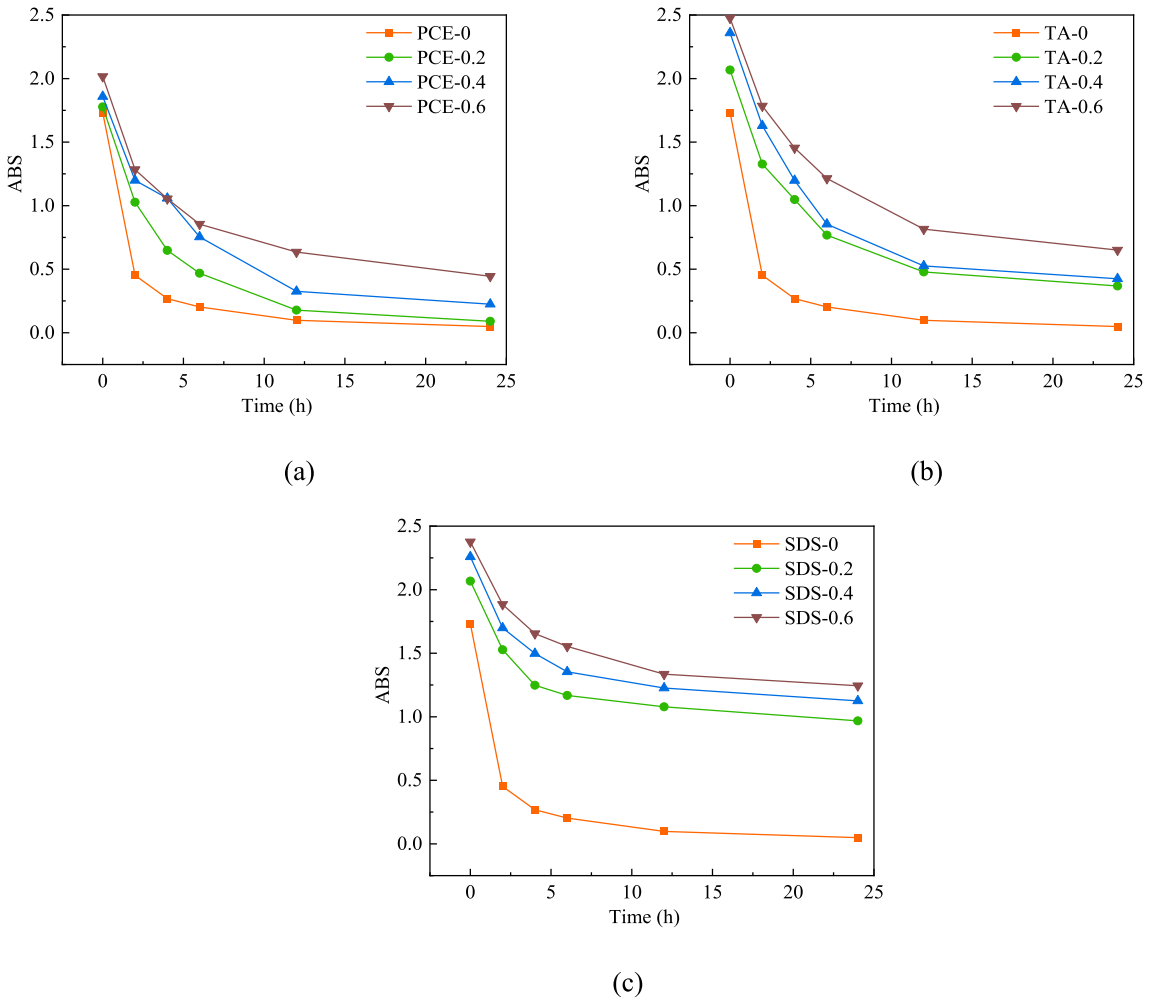


FIGURE 2
ABS *versus* time **(A)** PCE, **(B)** TA and **(C)** SDS.

accelerated the hardening process of cement. This may be because SDS was unable to form a complex with calcium ions, its main role was to prevent NCB agglomeration, and the interaction with the cement paste was weak.

## 3.3 Mechanical properties of NC

### 3.3.1 Flexural strength

Figures 4A–C show the flexural strength of NC with different PCE, TA and SDS contents at early hydration stage (3 days) and late hydration stage (28 days), respectively. As can be seen from the figure, the flexural strength of NC without dispersant at 3 days and 28 days was 5.2 MPa and 7.2 MPa, respectively. The flexural strength of NC after adding dispersant was higher than that of the sample without dispersant in the early and late stages of hydration, indicating that the three dispersants all increased the flexural strength to varying degrees, and showed a trend of first increasing and then decreasing.

With the increase of PCE content, the flexural strength of PCE-0.2, PCE-0.4 and PCE-0.6 increased by 32.7%, 26.9% and 7.7%, respectively, compared with that of PCE-0 at 3 days. The early flexural strength of NC was improved best when the content of PCE was 0.2%. At 28 days, the flexural strength of CPE-0.2, CPE-0.4 and CPE-0.6 increased by 19.4%, 16.7% and 12.5%, respectively, indicating that the influence of PCE content on the flexural strength at the later stage of hydration was small, which may be due to the delay of hydration of cement particles coated by PCE in the early stage and the gradual release of cement particles in the later stage. The difference in flexural strength was reduced. Their behavior was different. At 3 days, the flexural strength of TA-0.2, TA-0.4 and TA-0.6 increased by 5.8%, 13.5% and 3.8% compared with TA-0, respectively, indicating that 0.4% TA content contributed the most to the early flexural strength of NC. However, the flexural strength changes of TA-0.2, TA-0.4 and TA-0.6 at 28 days were 0%, 8.3% and −4.2%, respectively, indicating that too much TA was not beneficial to the growth of flexural strength, which may be related to its retarding effect. For SDS, the flexural strength of SDS-0.2, SDS-0.4 and SDS-0.6 increased by 15.4%, 19.2% and 5.8%, respectively,

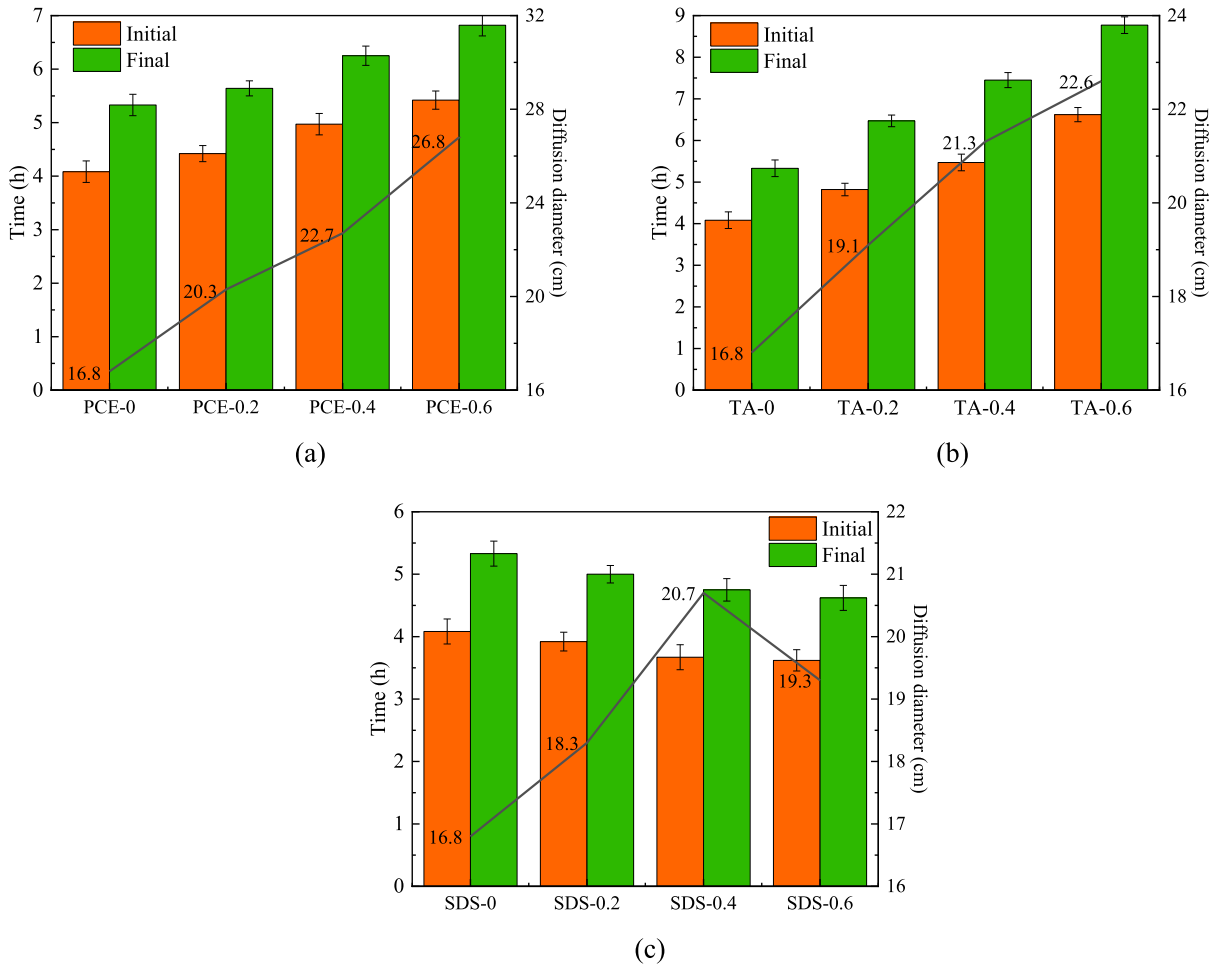


FIGURE 3
Fresh NC fluidity and setting time **(A)** PCE, **(B)** TA and **(C)** SDS.

compared with SDS-0 at 3 days, indicating that 0.4% SDS content contributed the most to the early flexural strength. At 28 days, the flexural strength increased by 8.3%, 12.5% and 1.4%, respectively.

### 3.3.2 Compressive strength

Figures 5A–C show the compressive strength of NC with different PCE, TA and SDS contents at early hydration stage (3 days) and late hydration stage (28 days), respectively. As can be seen from the figure, the compressive strength of NC without dispersant at 3 days and 28 days was 22.3 MPa and 32.6 MPa, respectively. The law of compressive strength was the same as that of flexural strength mentioned above.

As for PCE, the compressive strength of PCE-0.2, PCE-0.4 and PCE-0.6 at 3 days increased by 37.7%, 27.8% and 14.3%, respectively, compared with that of PCE-0, with the increase of PCE-0.2 on the early compressive strength being the most significant. At 28 days, the compressive strength of CPE-0.2, CPE-0.4 and CPE-0.6 increased by 34.4%, 30.9% and 20.2%, respectively, compared with that of CPE-0, indicating that PCE had a significant effect on the compressive strength of NC, especially CPE-0.2 and CPE-0.4. This may be due to the fact that PCE improved paste fluidity, reduced internal bubbles and pores, and enhanced compressive strength. However, excessive PCE can cause retardation and segregation, leading to negative effects. The influence trend of TA and SDS on compressive strength was similar, and both reached the peak value when the dosage was 0.4%. Without dispersant, NCB easily aggregated in cement and reduced compressive strength. In TA-0.4 and SDS-0.4 samples, uniformly dispersed NCB promoted the nucleation of hydration products and improved the structural densification, thus enhancing compressive strength. However, excessive TA and SDS will increase the internal defects of the paste and reduce the compressive strength.

## 3.4 Resistivity of NC

Figures 6A–C show the resistivity of NC with different PCE, TA and SDS contents in early hydration (3 days) and late hydration (28 days), respectively. It can be seen from the figure that the resistivity of NC without dispersant was 8.31 MPa and 8.54 MPa at 3 days and 28 days, respectively. The reason for the increase of resistivity in the late hydration period was the loss of pore water, which reduced the electron conduction path. In general, the resistivity of NC mixed with dispersant was higher than that of samples without dispersant in the early and late stages

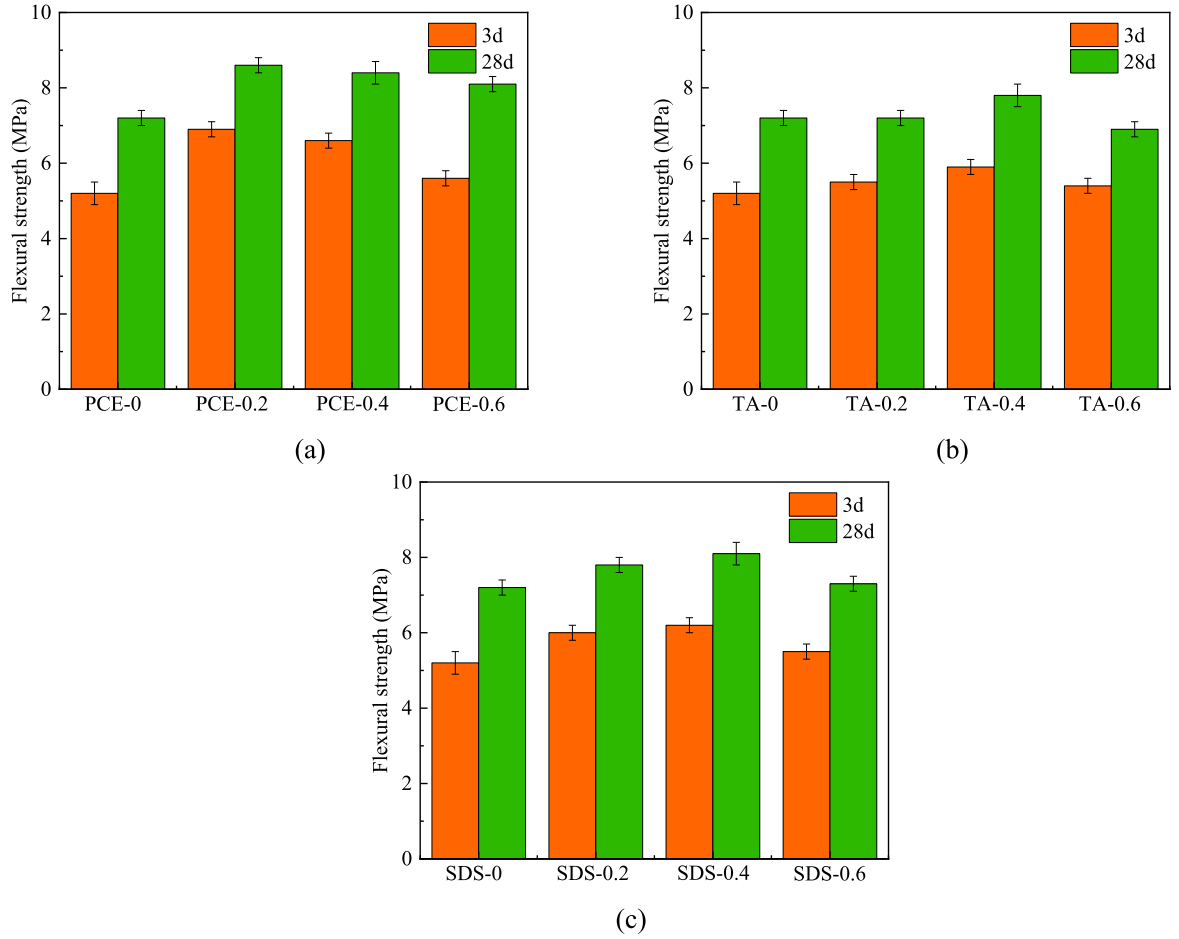


FIGURE 4
The flexural strength of NC **(A)** PCE, **(B)** TA, and **(C)** SDS.

of hydration, indicating that the three dispersants reduced the resistivity to different degrees, and the resistivity showed a trend of first decreasing and then increasing.

For PCE, the resistivity of PCE-0.2, PCE-0.4 and PCE-0.6 at 3 days decreased by 9.3%, 7.5% and 6.3%, respectively, as the content of PCE increased. When the PCE content was 0.2%, it made the greatest contribution to the reduction of the early resistivity of NC. At 28 days, the resistivity of CPE-0.2, CPE-0.4 and CPE-0.6 decreased by 10.4%, 7.4% and 6.6%, respectively, similar to the reduction in the early stage of hydration. The effect of PCE-0.2 was the best, but too much incorporation would lead to slow solidification and segregation of cement paste, which was not conducive to the performance of cement paste. For TA, the resistivity of TA-0.2, TA-0.4 and TA-0.6 decreased by 17.5%, 23.5% and 19.8% in 3 days compared with that of TA-0, respectively, and the best effect was achieved when the content of TA was 0.4%. At 28 days, the decrease of resistivity was basically the same as that at 3 days, and too much TA inclusion would increase the internal defects of the cement paste, resulting in an increase in resistivity. For SDS, the resistivity of SDS-0.2, SDS-0.4 and SDS-0.6 at 3 days was reduced by 11.3%, 17.3% and 11.2%, respectively, compared to SDS-0. With the increase of SDS content, the dispersion effect of NCB in cement was enhanced, and the resistance decreased first and then increased, reaching the lowest value at SDS-0.4. However, the high content of SDS would increase the porosity of cement matrix, but increased the resistivity.

With the increase of hydration time, the resistivity of the samples with different dispersants increased, but the overall trend remained unchanged. The reason was that the cement hydration was not complete in the early stage, and the resistivity of NC was affected by two aspects: First, NCB formed a conductive network conducive to electron transport in the cement matrix; The second was the conduction of electrons and ions in the pore liquid. At 28 days, the hydration of cement was basically completed, the pore liquid was reduced, and the electrical conductivity of ions was weakened, resulting in an increase in resistivity (He et al., 2018).

## 3.5 Microscopic characterization of NC

### 3.5.1 Types of hydration products

The XRD patterns displayed in Figure 7 provide a comparative analysis of the hydration products formed in the samples PCE-0.4, TA-0.4, SDS-0.4, and the Ctrl. The crystalline hydration products identified in the NC were $Ca(OH)_2$, $CaCO_3$, and $CaSO_4$.

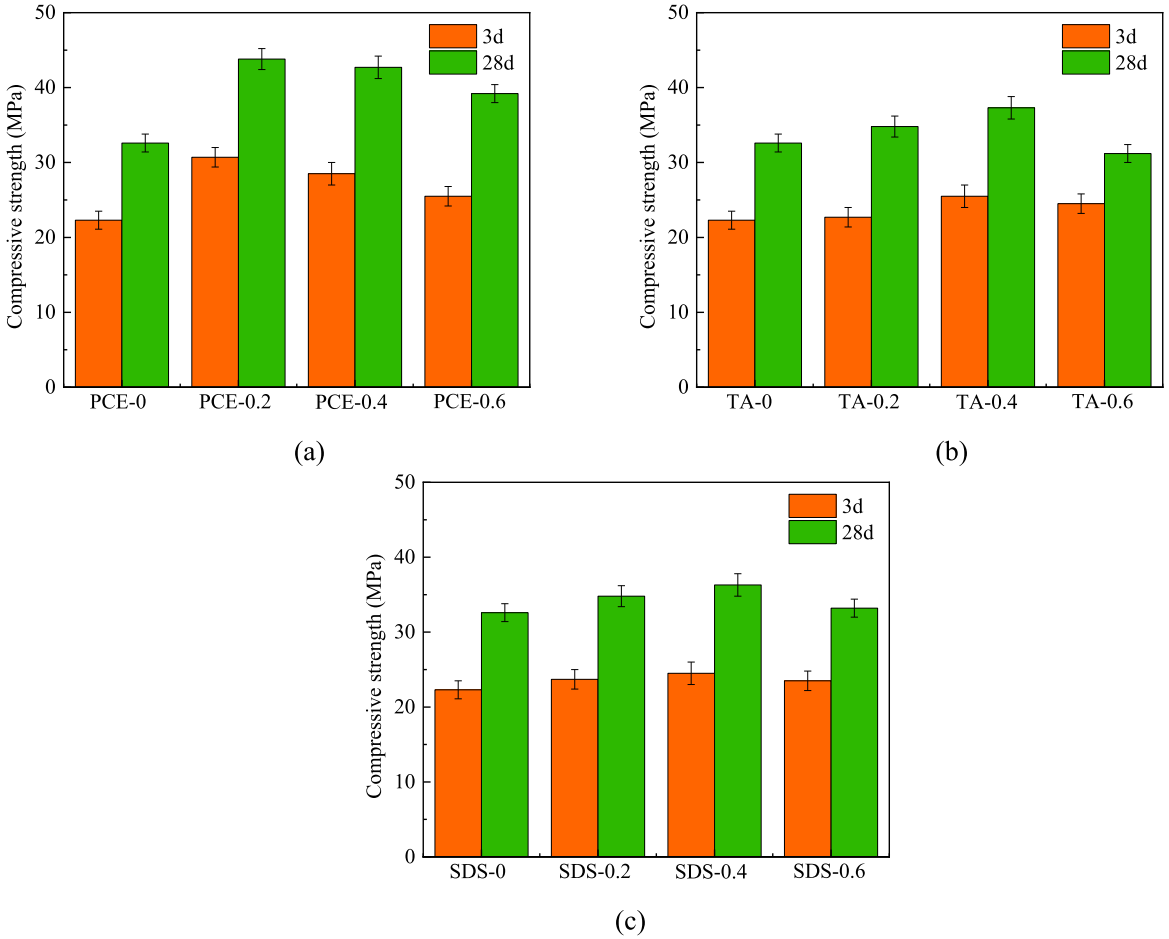


FIGURE 5
The compressive strength of NC **(A)** PCE, **(B)** TA, and **(C)** SDS.

It was noteworthy that the introduction of various dispersants, PCE, TA, and SDS, did not appear to alter the fundamental types of hydration products generated during the hydration process. This indicated that while the dispersants may play a role in improving the dispersion and workability of the NCB, they did not influence the chemical composition of the hydration products.

### 3.5.2 Distribution and morphology of hydration products

SEM images revealed the effect of NCB on the microstructure of the cement paste. As shown in Figure 8, the dispersion of NCB under SEM significantly affected the characteristics of the cement paste. In Figure 8A, the hydration products of NCB were sparsely distributed. This distribution was mainly due to the high surface energy of NCB itself and the lack of sufficient dispersant, which made it difficult to combine with cement particles, thus limiting its promotion effect on hydration. Some incomplete granular products were unevenly dispersed and not tightly connected. As a result, unmodified NCB may form new pores and defects in the cement, reducing the fluidity of the material and the compactness of the overall structure. With the addition of SDS dispersant, as shown in Figure 8B, the agglomeration of NCB in cement almost disappeared. The dispersed particles exhibited a uniform and continuous network distribution, which helped to promote the formation of C-S-H. At the same time, the hydration product was wrapped on the surface of NCB, which increased the crystallization degree of the hydration product, filled the micropores, and improved the compactness of the cement. NCB was surrounded by hydration products and acts as a nucleation site for C-S-H (Lu et al., 2019; Chen et al., 2024), facilitating the formation of a more dense and homogeneous cement structure. In Figure 8C, the distribution of AFt and C-S-H appeared sparse and porous, while in Figure 8D, these products were clustered in cement. This aggregation effectively enhanced the mechanical strength and conductivity of the cement paste, indicating that SDS had successfully achieved the dispersion of NCB in the cement paste. Through the uniformly dispersed NCB, a conductive network was formed, and the tightness of the connection between the hydration products was improved, which provided a preliminary explanation for the improvement of SDS-0.4 in terms of mechanical strength and resistivity. This improvement may be due to the effect of SDS on the interaction between cement particles and NCB, which promoted the effective dispersion of NCB and optimized the microstructure of cement paste.

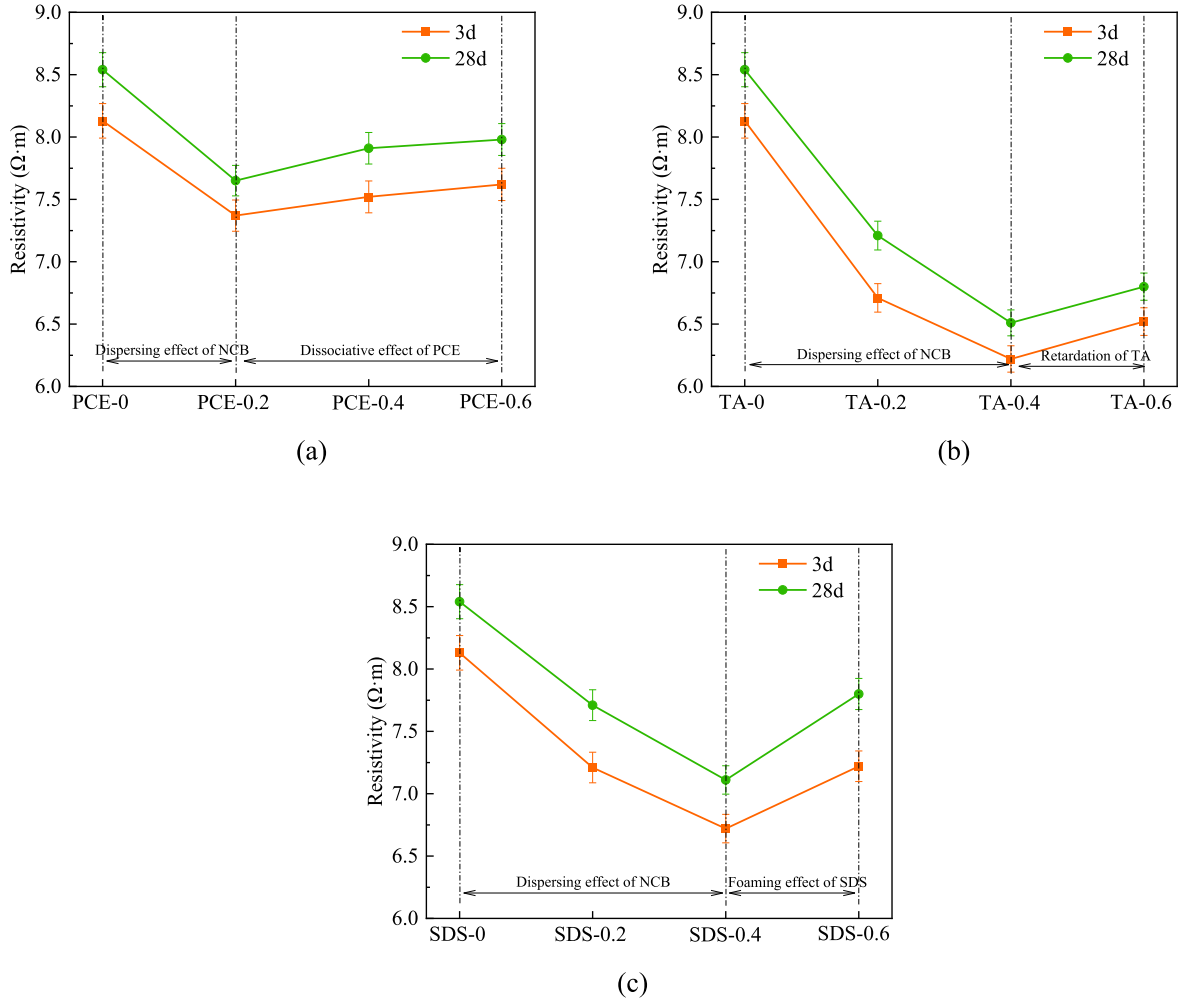


FIGURE 6
Resistivity of NC **(A)** PCE, **(B)** TA, and **(C)** SDS.

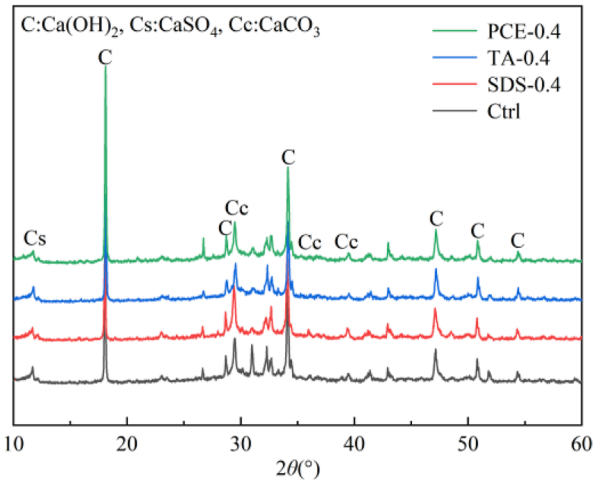


FIGURE 7
XRD of SDS-0 and SDS-0.4.

## 3.6 Snow-melting speed of NC

As shown in the Figure 9, the addition of three dispersants accelerated the snow-melting rate of NC to different degrees. Among them, TA had the most obvious effect, and the time can be reduced to 1/3; SDS followed, and PCE had the weakest effect. In the TA group, the decrease rate of TA-0.4 was the highest, the optimal dosage of SDS was also 0.4, and the optimal dosage of PCE was 0.2. The results were consistent with the resistivity results. The effect of dispersant directly affected the uniform distribution of NCB in the paste. The better the dispersion effect, the more uniform the distribution of NCB in the cement hardened paste, the lower the resistance, the better the conductivity, the higher the ice melting efficiency, and the lower the energy consumption. The reduction in electricity consumption of the TA group directly led to a reduction in $CO_2$ emissions.

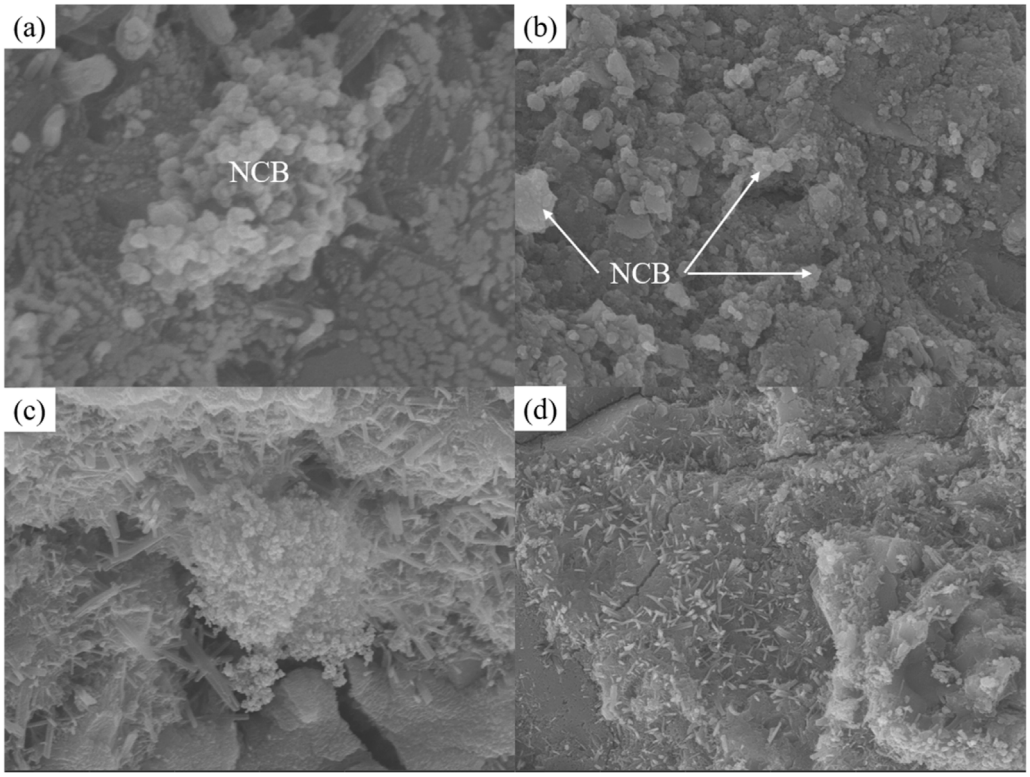


FIGURE 8
SEM of **(A) (C)** SDS-0 and **(B) (D)** SDS-0.4.

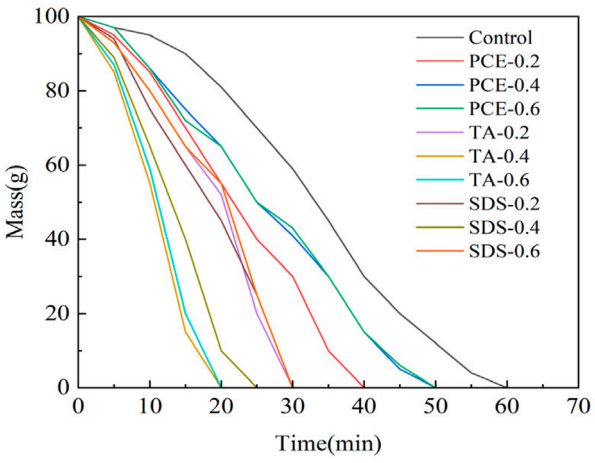


FIGURE 9
Ice mass loss of NC with different dispersants.

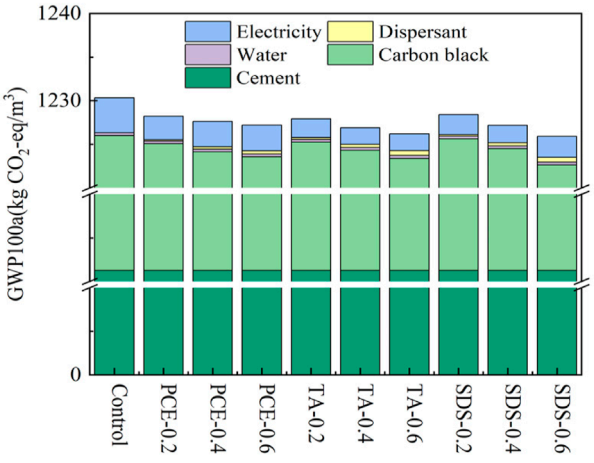


FIGURE 10
NC environmental impact assessment.

## 3.7 LCA analysis

Figure 10 shows GWP100a values of NC with different PCE, TA and SDS contents. The $CO_2$ emissions of NC was mainly concentrated in cement and carbon black. Secondly, it was the electric energy required in the snow-melting process, it can be found that the electric energy of TA was the least, mainly because TA improved the ice melting efficiency of NC, SDS was in the middle, and the NC with PCE had the highest snow-melting energy consumption. $CO_2$ was the main pollutant causing global warming, so while improving the efficiency of snow-melting and deicing of cement paste, carbon emissions should also be controlled.

According to the comprehensive analysis, the impact of NCB on the environmental load of cement paste is as follows: PCE was the largest, SDS was the second, TA was the least. In conclusion, the $CO_2$ emissions of NC with TA were the lowest.

## 4 Conclusion

In order to solve the problem of poor dispersion of NCB in cement paste and low snow-melting efficiency of NC, three dispersants, PCE, TA and SDS, were used in this paper to modify NC, which not only improved its dispersion, but also enhanced its mechanical and electrical properties, reduced $CO_2$ emissions of NC. Meanwhile, snow-melting speed and life cycle assessment analysis of NC with different dispersants were investigated. The main conclusions are as follows:

(1) All three dispersants can improve the dispersion stability of NCB suspension. PCE improved the dispersion stability of NCB suspension the least, the effect of TA and SDS was similar. Under the same dosage, PCE had the most significant improvement on fluidity, TA was the second, SDS was the least. PCE and TA both delayed the setting time, TA effect was more obvious, while SDS shortened the setting time.

(2) The influence of PCE, TA and SDS on the compressive and flexural strength of NC was similar, which firstly increased and then decreased. The three dispersants all improved the mechanical strength of NC to varying degrees. The highest contribution to the mechanical strength was PCE-0.2, TA-0.4 and SDS-0.4, respectively.

(3) The three dispersants can reduce the resistivity of NC at different hydration stages, and showed a trend of first decreasing and then increasing. PCE-0.2 can effectively reduce the resistivity of the sample, but excessive use will cause retarding and segregation, resulting in increased resistivity. TA-0.4 had the best effect on the improvement of resistivity, reducing the resistivity by 23.8% at 28 days, but excess can also cause retarding and increased resistivity. SDS-0.4 can minimize the resistivity, but excessive will lead to foaming and increase the porosity of the cement matrix.

(4) The three dispersants all accelerated the snow-melting speed of NC by dispersing NCB, among which the snow-melting speed of NC with TA was the fastest. From the perspective of global warming potential, the three dispersants all reduced the $CO_2$ emissions of NC. The impact of different dispersants NC on environmental load is as follows: PCE had the largest impact, followed by SDS, and TA had the least impact.

In this paper, low cost and high conductivity NCB was used to modify the cement paste, and the advantages of the structure and performance of the material were used in the test and the ideal results were obtained. Subsequently, the thermal conductivity of composite materials can be studied to provide a new idea for road deicing and snow removal in northern and western high-altitude areas in winter.

## Data availability statement

The original contributions presented in the study are included in the article/supplementary material, further inquiries can be directed to the corresponding author.

## Author contributions

HW: Conceptualization, Methodology, Writing–original draft. CL: Data curation, Investigation, Writing–original draft. HG: Software, Supervision, Writing–original draft. YZ: Formal Analysis, Investigation, Writing–review and editing. HX: Supervision, Validation, Writing–review and editing. CZ: Methodology, Supervision, Writing–review and editing. SZ: Investigation, Methodology, Writing–review and editing. QZ: Conceptualization, Funding acquisition, Writing–review and editing.

## Funding

The author(s) declare that financial support was received for the research, authorship, and/or publication of this article. This study was financially supported by the National Joint Foundation for Regional Innovation and Development of China (U22A20228).

## Conflict of interest

Authors HW, HG, and CZ were employed by Cangzhou Qugang Expressway Construction Co., Ltd. Authors YZ and HX were employed by China Mcc22 Group Corporation Ltd. Author SZ was employed by Fujian Zhanglong Construction Investment Group Co., Ltd.

The remaining authors declare that the research was conducted in the absence of any commercial or financial relationships that could be construed as a potential conflict of interest.

## Generative AI statement

The author(s) declare that no Generative AI was used in the creation of this manuscript.

## Publisher's note

# References


Bai, S., Jiang, L., Xu, N., Jin, M., and Jiang, S. (2018). Enhancement of mechanical and electrical properties of graphene/cement composite due to improved dispersion of graphene by addition of silica fume. *Constr. Build. Mater.* 164, 433–441. doi:10.1016/j.conbuildmat.2017.12.176

Chen, X., Liu, T., Guo, J., Nie, K., Yang, X., Zhang, L., et al. (2024). C–S–H-PCE nanoparticles and anionic surfactants as nucleation agent in cement based materials: focus on the antagonism. *Cem. Concr. Compos.* 152, 105644. doi:10.1016/j.cemconcomp.2024.105644

Chuah, S., Li, W., Chen, S. J., Sanjayan, J. G., and Duan, W. H. (2018). Investigation on dispersion of graphene oxide in cement composite using different surfactant treatments. *Constr. Build. Mater.* 161, 519–527. doi:10.1016/j.conbuildmat.2017.11.154

Geim, A. K., and Novoselov, K. S. (2007). The rise of graphene. *Nat. Mater.* 6 (3), 183–191. doi:10.1038/nmat1849

Gong, H., Li, Z., Zhang, Y., and Fan, R. (2009). Piezoelectric and dielectric behavior of 0-3 cement-based composites mixed with carbon black. *J. Eur. Ceram. Soc.* 29 (10), 2013–2019. doi:10.1016/j.jeurceramsoc.2008.11.014

Han, B., Zhang, L., Sun, S., Yu, X., Dong, X., Wu, T., et al. (2015). Electrostatic self-assembled carbon nanotube/nano carbon black composite fillers reinforced cement-based materials with multifunctionality. *Compos. Part A Appl. Sci. Manuf.* 79, 103–115. doi:10.1016/j.compositesa.2015.09.016

He, R., Ma, H., Hafiz, R. B., Fu, C., Jin, X., and He, J. (2018). Determining porosity and pore network connectivity of cement-based materials by a modified non-contact electrical resistivity measurement: experiment and theory. *Mater. and Des.* 156, 82–92. doi:10.1016/j.matdes.2018.06.045

Hong, Y., Li, Z., Qiao, G., Ou, J., and Cheng, W. (2018). Pressure sensitivity of multiscale carbon-admixtures–enhanced cement-based composites. *Nanomater. Nanotechnol.* 8, 184798041879352. doi:10.1177/1847980418793529

Huang, K., Liu, J., Wang, J., and Shi, X. (2021). Characterization and mechanism of a new superhydrophobic deicing coating used for road pavement. *Crystals* 11, 1304. doi:10.3390/cryst11111304

Julitta, T., Cremonese, E., Migliavacca, M., Colombo, R., Galvagno, M., Siniscalco, C., et al. (2014). Using digital camera images to analyse snowmelt and phenology of a subalpine grassland. *Agric. For. Meteorology* 198-199, 116–125. doi:10.1016/j.agrformet.2014.08.007

Keal, M. E., Clewlow, L., Roberts, E., and Rees, N. V. (2024). Electrochemical recovery of ruthenium via carbon black nano-impacts. *Electrochimica Acta* 507, 145185. doi:10.1016/j.electacta.2024.145185

Kishore, K., Pandey, A., Wagri, N. K., Saxena, A., Patel, J., and Al-Fakih, A. (2023). Technological challenges in nanoparticle-modified geopolymer concrete: a comprehensive review on nanomaterial dispersion, characterization techniques and its mechanical properties. *Case Stud. Constr. Mater.* 19, e02265. doi:10.1016/j.cscm.2023.e02265

Lavagna, L., Nisticò, R., Musso, S., and Pavese, M. (2021). Functionalization as a way to enhance dispersion of carbon nanotubes in matrices: a review. *Mater. Today Chem.* 20, 100477. doi:10.1016/j.mtchem.2021.100477

Li, G., Qin, J.-m., Yu, H.-x., and Huang, N. (2022). Wind-tunnel experimental studies of the spatial snow distribution over grass and bush surfaces. *J. Hydrodynamics* 34 (1), 85–93. doi:10.1007/s42241-022-0009-4

Li, H., Zhang, Q. Q., and Xiao, H. G. (2013). Self-deicing road system with a CNFP high-efficiency thermal source and MWCNT/cement-based high-thermal conductive composites. *Cold Regions Sci. Technol.* 86, 22–35. doi:10.1016/j.coldregions.2012.10.007

liu, X., Song, A., Chen, S., Li, Q., Sun, R., Yang, J., et al. (2019). Conductive mechanism of CNTs enhanced conductive magnetic fluid. *Mater. Lett.* 252, 110–113. doi:10.1016/j.matlet.2019.05.088

Lu, Z., Chen, B., Leung, C. Y., Li, Z., and Sun, G. (2019). Aggregation size effect of graphene oxide on its reinforcing efficiency to cement-based materials. *Cem. Concr. Compos.* 100, 85–91. doi:10.1016/j.cemconcomp.2019.04.005

Ma, T., Geng, L., Ding, X., Zhang, D., and Huang, X. (2016). Experimental study of deicing asphalt mixture with anti-icing additives. *Constr. Build. Mater.* 127, 653–662. doi:10.1016/j.conbuildmat.2016.10.018

Nan, Z., Ma, P., Yang, Z., Fang, Y., and Zhang, Z. (2023). Physical dispersion method and mechanism of graphene. *J. Superhard Mater.* 45 (3), 186–191. doi:10.3103/s1063457623030218

Nayır, S., Bahadır, Ü., and Toğan, V. (2024). Investigation of global warming potential of concrete with silica fume and blast furnace slag. *Iran. J. Sci. Technol. Trans. Civ. Eng.* 48 (4), 1965–1975. doi:10.1007/s40996-023-01264-x

Pan, H., She, W., Zuo, W., Zhou, Y., Huang, J., Zhang, Z., et al. (2020). Hierarchical toughening of a biomimetic bulk cement composite. *ACS Appl. Mater. and Interfaces* 12 (47), 53297–53309. doi:10.1021/acsami.0c15313

Pei, Z., Yi, J., Li, Y., Cheng, P., Zhu, Y., and Feng, D. (2021). Material design and performance analysis of the anti-ice and antiskid wear layer on pavement. *Constr. Build. Mater.* 282, 122734. doi:10.1016/j.conbuildmat.2021.122734

Pytka, J. (2010). Determination of snow stresses under vehicle loads. *Cold Regions Sci. Technol.* 60 (2), 137–145. doi:10.1016/j.coldregions.2009.10.002

Sobolkina, A., Mechtcherine, V., Khavrus, V., Maier, D., Mende, M., Ritschel, M., et al. (2012). Dispersion of carbon nanotubes and its influence on the mechanical properties of the cement matrix. *Cem. Concr. Compos.* 34 (10), 1104–1113. doi:10.1016/j.cemconcomp.2012.07.008

Sokołowska, J. J., Łukowski, P., and Bączek, A. (2024). Mortars with polypropylene fibers modified with tannic acid to increase their adhesion to cement matrices. *Appl. Sci.* 14, 2677. doi:10.3390/app14072677

Wang, T., Dra, Y. A. S. S., Cai, X., Cheng, Z., Zhang, D., Lin, Y., et al. (2022). Advanced cold patching materials (CPMs) for asphalt pavement pothole rehabilitation: state of the art. *J. Clean. Prod.* 366, 133001. doi:10.1016/j.jclepro.2022.133001

Xu, S., Zhou, Z., Feng, L., Cui, N., and Xie, N. (2021). Durability of pavement materials with exposure to various anti-icing strategies. *Processes* 9, 291. doi:10.3390/pr9020291

Xu, Y., Zeng, J., Chen, W., Jin, R., Li, B., and Pan, Z. (2018). A holistic review of cement composites reinforced with graphene oxide. *Constr. Build. Mater.* 171, 291–302. doi:10.1016/j.conbuildmat.2018.03.147

Yıldırım, G., Sarwary, M. H., Al-Dahawi, A., Öztürk, O., Anıl, Ö., and Şahmaran, M. (2018). Piezoresistive behavior of CF- and CNT-based reinforced concrete beams subjected to static flexural loading: shear failure investigation. *Constr. Build. Mater.* 168, 266–279. doi:10.1016/j.conbuildmat.2018.02.124

Yoo, D.-Y., You, I., and Lee, S.-J. (2017). Electrical properties of cement-based composites with carbon nanotubes, graphene, and graphite nanofibers. *Sensors* 17, 1064. doi:10.3390/s17051064

Zhai, S., Zhou, X., Zhang, Y., Pang, B., Liu, G., Zhang, L., et al. (2023). Effect of multifunctional modification of waste rubber powder on the workability and mechanical behavior of cement-based materials. *Constr. Build. Mater.* 363, 129880. doi:10.1016/j.conbuildmat.2022.129880

Zhan, M., Pan, G., Zhou, F., Mi, R., and Shah, S. P. (2020). *In situ*-grown carbon nanotubes enhanced cement-based materials with multifunctionality. *Cem. Concr. Compos.* 108, 103518. doi:10.1016/j.cemconcomp.2020.103518

Zhao, X., Zhang, Y., and Zheng, M. (2024). Enhancing the efficiency of ice-resistant materials in asphalt road surfaces: a comprehensive performance analysis. *Coatings* 14, 37. doi:10.3390/coatings14010037

Zhu, Y., Murali, S., Cai, W., Li, X., Suk, J. W., Potts, J. R., et al. (2010). Graphene and graphene oxide: synthesis, properties, and applications. *Adv. Mater.* 22 (35), 3906–3924. doi:10.1002/adma.201001068